

# Design of an innovative exoskeletal forearm-wrist mechanism

Philippe Garrec, Alexandre Verney

► **To cite this version:**

Philippe Garrec, Alexandre Verney. Design of an innovative exoskeletal forearm-wrist mechanism. ICABB 2010: 1st International Conference on Applied Bionics and Biomechanics, Oct 2010, Venise, Italy. cea-01144016

**HAL Id: cea-01144016**

**<https://hal-cea.archives-ouvertes.fr/cea-01144016>**

Submitted on 20 Apr 2015

**HAL** is a multi-disciplinary open access archive for the deposit and dissemination of scientific research documents, whether they are published or not. The documents may come from teaching and research institutions in France or abroad, or from public or private research centers.

L'archive ouverte pluridisciplinaire **HAL**, est destinée au dépôt et à la diffusion de documents scientifiques de niveau recherche, publiés ou non, émanant des établissements d'enseignement et de recherche français ou étrangers, des laboratoires publics ou privés.

# Design of an innovative exoskeletal forearm-wrist mechanism

Philippe Garrec, Alexandre Verney (1)

**Abstract** — This paper presents an innovative 3-joints structure designed as the forearm-wrist of a force controlled exoskeleton. It is composed of an open parallel mechanism both fitting the human forearm and able to rotate on its longitudinal joint (prono-supination), in a similar manner of the ulna-radius movement. This structure advantageously replaces circular guidings in terms of mass, volume and friction and can be freely scaled. A lightweight 3 dof forearm-wrist mechanism is proposed as an integral rotation module for the general-purpose arm exoskeleton ABLE 7 D.

## I. INTRODUCTION

THIS document presents the design of the forearm-wrist module [9], with a focus on the cable

transmission of the Screw-Cable-System [2] driving the prono-supination movement. Exact modeling and computing of the driving pulley is presented. The two complementary joints of the wrist, also actuated by SCS, are briefly presented.

## II. FOREARM WITH PRONO-SUPINATION

### A. Articulated structure

A scheme of the forearm mechanism is given Fig. 1.

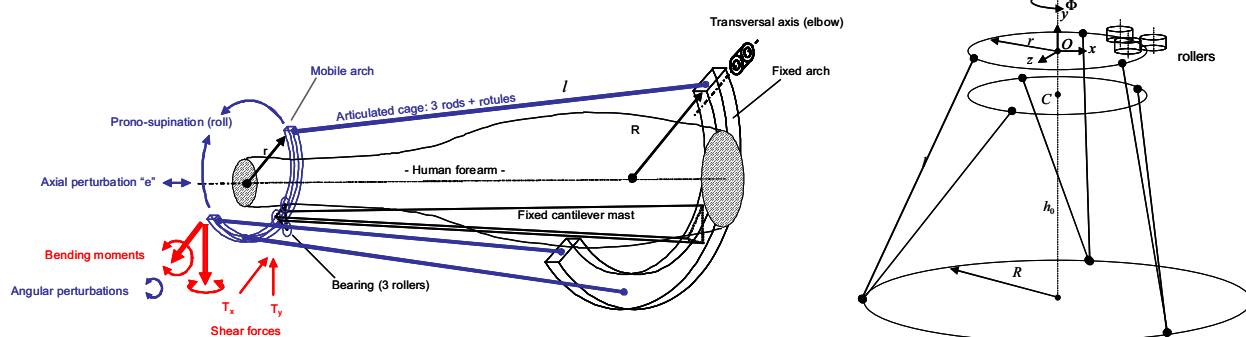


Fig. 1. Left, Forearm parallel mechanism with prono-supination and decoupled bending moments / shear forces ; Right, its basic geometrical model

It combines a parallel structure made of at least 3 rods, connecting a mobile arch to a fixed arch thanks to ball-joints, and a fixed cantilever mast ensuring the circular motion of the mobile arch thanks to a set of 3 rollers. Such an articulated structure is achieving both a structural function and a circular guide function (axial rotation or prono-supination). Incidentally, this movement evokes those of the radius-ulna bones. Shear forces are balanced by the fixed cantilever mast whereas bending moments are balanced by traction/compression forces in the rods. Such a decoupling effect allows making an optimal use of each mechanical component: miniature bearings can easily sustain the desired shear forces (about 50 N) whereas lightweight rods/ball-joints can easily transmit the required traction/compression forces (about 150 N). For

all these reasons, compared to an existing industrial product such as THK HCR circular bearing or previous published designs [1],[4],[5],[8], such a mechanism offers a better compromise between volume, weight/inertia and friction and it can be more easily scaled to the person. It also preserves the openness of a circular bearing, a favorable factor for safety and acceptability.

The displacement law as a function of the prono-supination angle is given by (1).

$$y_C = \sqrt{h_0^2 + 2Rr(\cos \Phi - 1)} - h_0 \quad (1)$$

(1) Philippe Garrec ([philippe.garrec@cea.fr](mailto:philippe.garrec@cea.fr)) and Alexandre Verney ([alexandre.verney@cea.fr](mailto:alexandre.verney@cea.fr)) are with the CEA, LIST, Interactive Robotics Laboratory, Fontenay aux Roses, F- 92265, France

With:

$$l = \sqrt{(R-r)^2 + h_0^2}$$

$$y_c = \sqrt{h_0^2 + 2Rr(\cos \Phi - 1)} - h_0$$

$$\begin{cases} y(0) = 0 \\ y_{c_{\max}} = \sqrt{h_0^2 + 2Rr(\cos \Phi_{\max} - 1)} - h_0 \end{cases}$$

The rotation travel is limited either by interferences between the rods and the fixed parts or by the axial translation of the mobile arch. An order of magnitude of this translation for a pronation/supination of 60° is given in TABLE I.

TABLE I  
Estimated translation for a human forearm

Angular travel		120°
Pronation / Supination	$\Phi_{\max}$	60°
Fixed arch radius	R	60mm
Mobile arch radius	r	60mm
Nominal distance between arches	$h_0$	250mm
Rod length	l	250mm
Maximum translation	$y_{C_{\max}}$	-7mm

In comparison with the flexibility of the skin and muscle, such a perturbation is relatively small (< 3%) and

is expected to be not detected by the user. A second cause of perturbation is the offset of the center C of the mobile arch (fabrication incertitude, play, elastic deflection under the load) which will induce an oscillation of its plane. In our current design Fig. 4, this amplitude is estimated at less than 1° which is virtually undetectable.

### B. Actuator

The translation of the arch represents an obvious challenge for the design of the drive. Because tests with gears did not provide a smooth torque transmission, we opted again for a SCS actuator. Its design had to be adapted to fit the geometrical constraints of the mast. The rotation of the screw is locked using a miniature ball-spline also used as a structural part of the mast. A flexible coupling connects its nut to an extremity of the screw. The screw delivers enough force to provide the required torque (approx. 2 Nm) without any gear reducer (Fig 2).

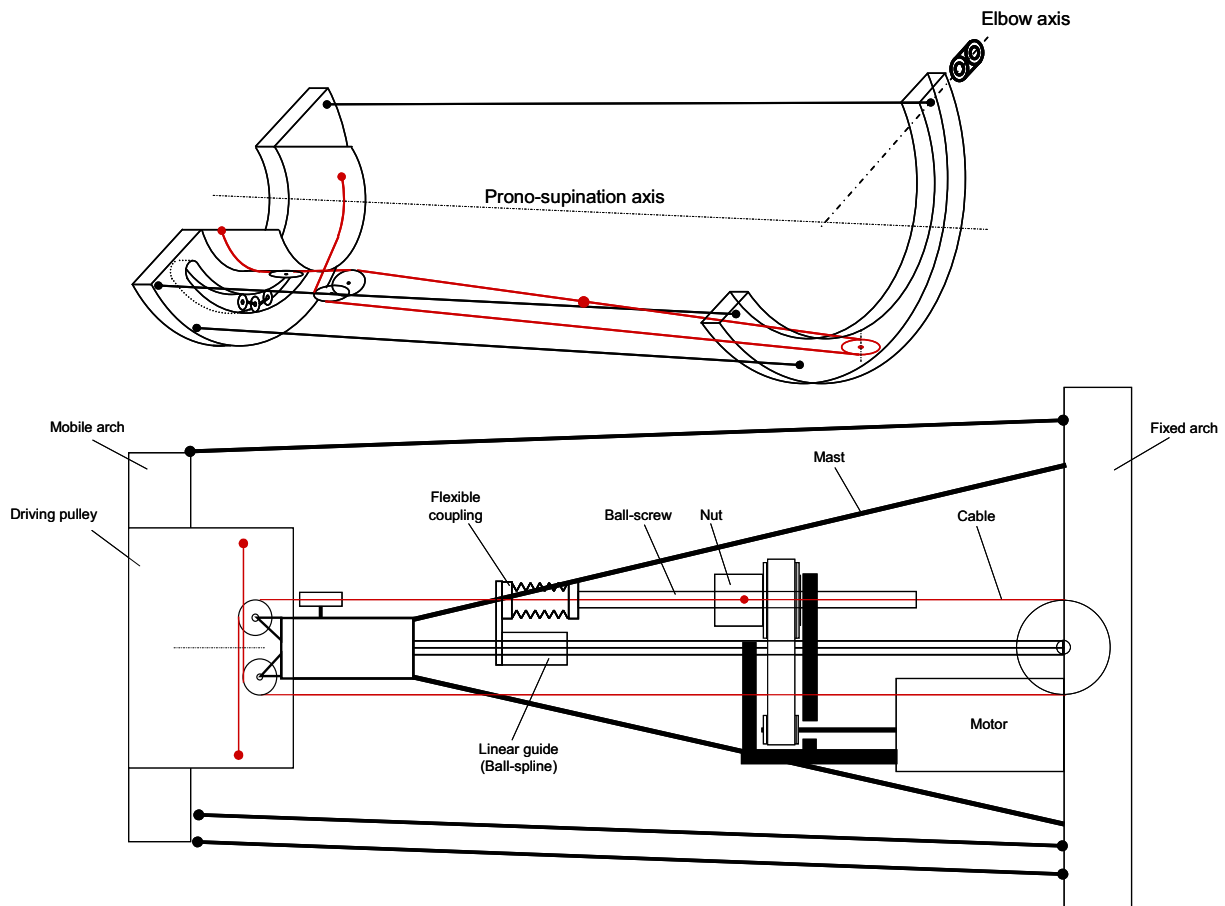


Fig 2. Prono-supination SCS actuator with details of the cable routing

Design of the driving pulley

Its rotation combined with a variable translation velocity

leads to a specific shape of the grooves. On the scheme Fig. 3, the spatial problem is transformed in a planar problem for simplicity (unfolded).

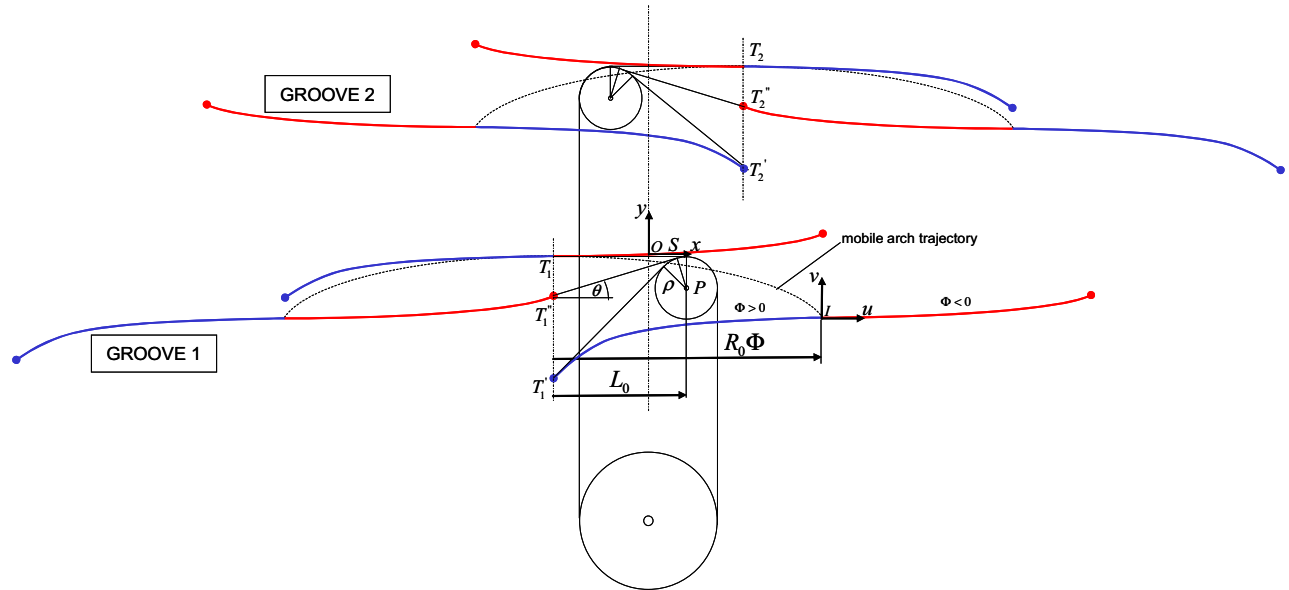


Fig. 3. Geometry of cable distribution on the driving pulley

The cable is deviated by the pulley  $P(p, q)$  and contacts the driving pulley in points  $T, T', T''$  (tangential line at the intersection of the deviating pulley plane and the driving pulley cylinder). There is a fixed frame  $(O, x, y)$ , with  $x$  representing the arc  $R\Phi$  and  $y$ , the translation of the mobile arch associated with the frame  $(I, u, v)$ . The origin of the groove  $I$  is such that for  $\Phi = 0$ ,  $I$  is confused with  $T$  where we also impose  $\theta = 0$ , leading to the following initial conditions:

$$v'(0) = v(0) = 0$$

The radius of the driving pulley is noted  $R_0$  and the distance between the deviating pulley center and the tangential line is noted  $L_0$ . For  $\Phi > 0$ , the cable is wrapped on the blue portion of the groove and on the red portion for  $\Phi < 0$ . Since the cable must ideally remain

constantly tangent to the groove at contact points  $T, T', T''$ , the groove presents different curvatures for both portions. On the alternate branch of the cable, the cable is wrapped on opposite portions of the second groove, due to the symmetry of the problem. By writing that the segment  $TS$  is the common tangent to the driving pulley and the deviating pulley, we obtain the following relations:

$$\frac{\rho(\cos\theta - 1) - y - v}{L_0 - \rho \sin\theta} = -R_0^{-1}v' = \text{tg}\theta \quad (2)$$

By using the trigonometric transformations:

$$\begin{cases} \cos\theta = (1 + R_0^{-2}v'^2)^{-1/2} \\ \sin\theta = (1 + R_0^2v'^{-2})^{-1/2} \end{cases}$$

we can eliminate  $\theta$  and finally obtain the non-linear differential equation (3) where  $v(\Phi)$  is the unknown function.

$$R_0^{-1}v' \left[ L_0 - \rho(1 + R_0^2v'^{-2})^{-1/2} \right] + \rho \left[ (1 + R_0^{-2}v'^2)^{-1/2} - 1 \right] - \sqrt{h_0^2 + 2Rr(\cos\Phi - 1)} - v = 0 \quad (3)$$

We solved it numerically by programming an Excel sheet, sampling the groove in 100 points. The computed results are presented below on Fig. 4 (coordinates

expressed in mm).

This study has been achieved within the frame of the French ANR (Agence Nationale de la Recherche) -

BRAHMA project which goal is to develop an upper limb exoskeleton for rehabilitation and assistance [6]. The grooves are milled with a 5 axis machine-tool using the

above computed data. Fig. 6 shows a CAD view and a picture of the prototype, equipped with adjustment devices.

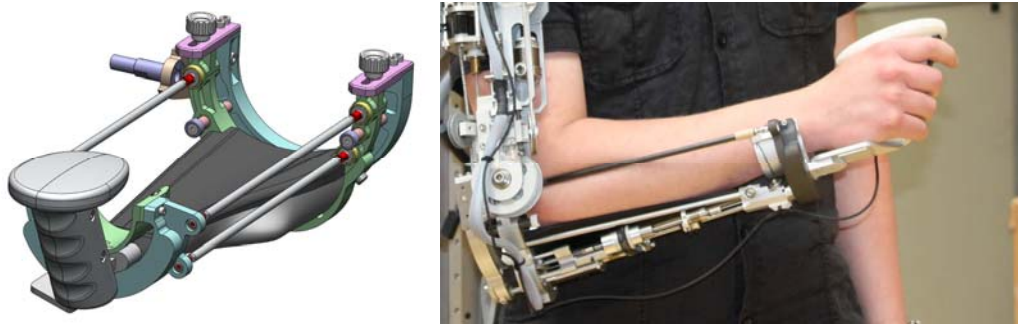
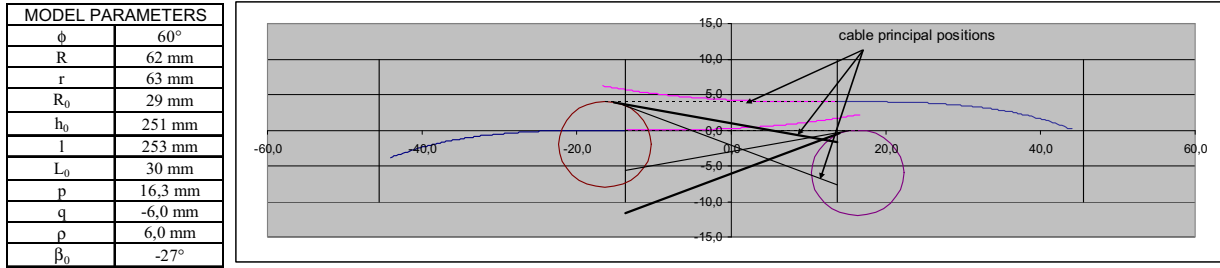


Fig. 4. Computation of the grooves (top) ; Views of the forearm prototype (bottom)

As a consequence, the reduction ratio varies asymmetrically apart the prono-supination origine (Fig. 5).

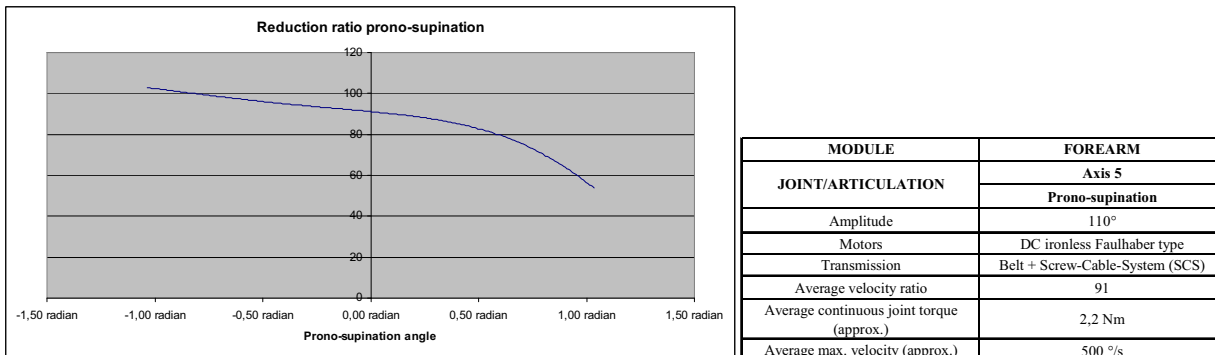


Fig. 5. Left, Reduction ratio law as a function of the prono-supination angle ; Right, provisional performances of the forerarm

Fig. 6 shows the forearm module integrated as the fifth joint of the ABLE arm exoskeleton [3],[7] to provide a cost-effective rehabilitation system whenever the medical benefits of a prono-supination movement are significant enough.



Fig. 6. CAD view of ABLE 5D arm exoskeleton

### III. FOREARM - WRIST STRUCTURE

The wrist is classically formed of two serial transversal and perpendicular axis (U-joint) attached to the mobile arch. Two SCS actuators are mounted on a structure that replaces one of the 3 rods (Fig 7). To ensure a proper routing of the cables, the attachment on the mobile arch is

achieved by two orthogonal articulations, each equipped with ad hoc deviation pulleys. The heterogeneous linkages on the mobile arch (two ball-joints and two orthogonal axis) causes some specific angular perturbations but of a low magnitude (below  $1^\circ$  for our design), a value compatible with the use of cable transmission for the prono-supination.

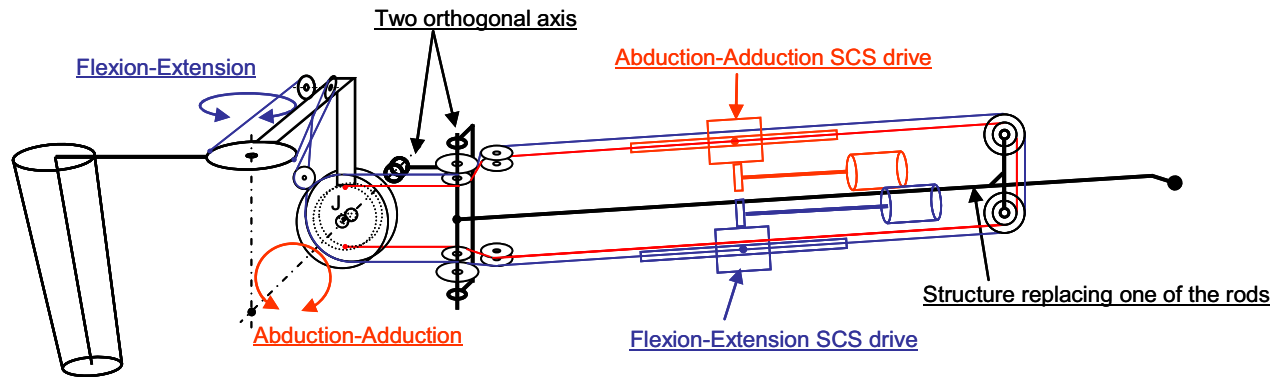


Fig 7. Wrist U-joint and its two SCS drives replacing one of the 3 rods of the forearm structure

There is a main linear coupling effect (red on blue) and complementary non-linear couplings of a low magnitude due to the variable inclination of the rods compared to the mobile arch. The alignment of the SCS actuators leads to a streamline shape and their reflected inertia around the prono-supination axis is even reduced because the velocity

decreases towards the fixed arch. Assembling the two preceding structures leads to a forearm-wrist module providing the required 3 orthogonal concurrent rotations. Fig 8 shows the end result and its integration in ABLE 7D arm exoskeleton.

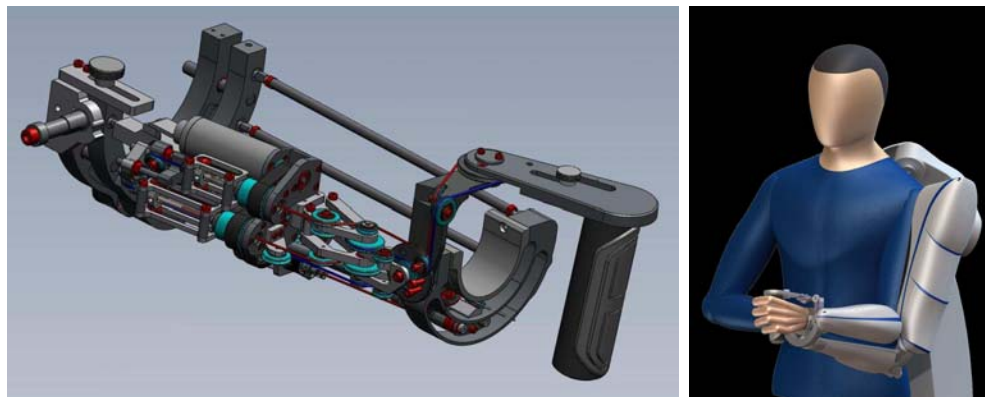


Fig 8. Right, Forearm - wrist 3 axis structure actuated by 3 SCS ; Left, Integration in ABLE 7D

This exoskeleton, is planned to be functional by the end of 2010 for the benefits of the ANR-SCALE 1 project which goal is to develop a full-size haptics system for the industry and for teleoperation.

### IV. CONCLUSION

A forearm-wrist module has been designed to present both a low friction/high efficiency and a particularly low inertia and total mass estimated of 2 kg. These unique characteristics open a broad field of applications where

force control is involved, including haptics. More work is still required to fully identify the non-linear models and control the performances to confirm the effectiveness of the design.

### REFERENCES

- [1] Bergamasco M., Allotta B., Bosio L., Ferretti L., Parrini G., Prisco G. M., Salsedo F., and Sartini G., "An arm exoskeleton system for teleoperation and virtual environments applications", in *Proc. IEEE Int. Conf. Robot. Autom.*, vol. 2, 1994, pp. 1449-1454
- [2] Garrec P., «Screw transmission, nut and cable attached to the screw» - Patent FR2809464

- [3] Garrec P., Martins J.P., Gravez, Perrot Y., Measson Y., "A New Force-Feedback, Morphologically Inspired Portable Exoskeleton" in *Proceedings of 15th IEEE International Symposium on Robot and Human Interactive Communication (RO-MAN - 2006)*, September 2006, Hatfield, UK.
- [4] J.C. Perry, J. Rosen, S. Burns, "Upper-Limb Powered Exoskeleton Design", *IEEE/ASME Transactions on Mechatronics*, Volume 12, Issue 4, Aug. 2007 Page(s):408 – 417
- [5] Frisoli L., Borelli A., Montagner, et al, "Arm rehabilitation with a robotic exoskeleton in Virtual Reality", *Proc. of IEEE ICORR 2007, Intern. Conf. on Rehabilitation Robotics*
- [6] N. Jarrassé, J. Robertson, P. Garrec, J. Paik, V. Pasqui, Y. Perrot, A. Roby-Brami, D. Wang, G. Morel, "Design and acceptability assessment of a new reversible orthosis", *Proceedings of IROS 2008, September 2008, Nice, France*.
- [7] Garrec P., Friconeau J. P., Méasson Y., Perrot Y., "ABLE, an Innovative Transparent Exoskeleton for the Upper-Limb", *Proceedings of IROS 2008, September 2008, Nice, France*.
- [8] Letier P., Avraam M., Veillerette S., Horodincea, M., De Bartolomei M., Schiele A. and Preumont A., "SAM : A 7-DOF Portable Arm Exoskeleton with Local Joint Control", *Proceedings of IROS 2008, September 2008, Nice, France*.
- [9] Garrec P., «Forearm rotation mechanism and orthosis including such mechanism"- Patent FR2917323